(23) W. W. Graessley and S. F. Edwards, *Polymer*, **22**, 1329 (1981).
(24) P. J. Flory, "Statistical Mechanics of Chain Molecules", Wiley-Interscience, New York, 1969.
(25) N. Hadjichristidis, Z. Xu, L. J. Fetters, and J. Roovers, *J. Polym. Sci., Polym. Phys. Ed.*, **20**, 743 (1982).
(26) G. Vinogradov, A. Malkin, Y. Yanovskii, E. Borisenkova, B. Yarlkov, and G. Berezhnaya, *J. Polym. Sci., Part A-2*, **10**, 1061 (1972).
(27) D. S. Pearson and W. W. Graessley, *Macromolecules*, **13**, 1001 (1980).
(28) B. J. R. Scholtens, *J. Polym. Sci., Polym. Phys. Ed.*, **22**, 317 (1984).
(29) W. W. Graessley, T. Masuda, J. E. L. Roovers, and N. Hadjichristidis, *Macromolecules*, **9**, 127 (1976).
(30) J. E. Mark, *J. Polym. Sci., Polym. Phys. Ed.*, **12**, 1207 (1974).
(31) J. M. Carella, Doctoral Thesis, Chemical Engineering Department, Northwestern University, 1983; J. M. Carella, W. W. Graessley, and L. J. Fetters, *Macromolecules*, following paper in this issue.
(32) G. Ronca, *J. Chem. Phys.*, **79**, 1031 (1983).

Effects of Chain Microstructure on the Viscoelastic Properties of Linear Polymer Melts: Polybutadienes and Hydrogenated Polybutadienes

José M. Carella[1a] and William W. Graessley*[1b]

Chemical Engineering Department, Northwestern University, Evanston, Illinois 60201

Lewis J. Fetters[1b]

Institute of Polymer Science, University of Akron, Akron, Ohio 44325.
Received May 9, 1984

ABSTRACT: Linear viscoelastic properties in the plateau and terminal regions were measured over wide ranges of temperature and chain microstructure in melts of polybutadiene and hydrogenated polybutadiene. All samples were linear with high molecular weights ($M \gg M_c$) and narrow distributions ($\bar{M}_w/\bar{M}_n < 1.1$). The polybutadienes vary in microstructure from 8% to 99% vinyl content; the hydrogenated polybutadienes are equivalent structurally to copolymers of ethylene with 4–99% 1-butene. Primary attention was given to properties that depend on chain microstructure but are insensitive to chain length for long chains—the plateau modulus $G_N°$, the steady-state recoverable compliance $J_e°$, and the temperature shift factors for the frequency and modulus, a_T and b_T. The microstructural effects on a_T reflect primarily the location of the glass transition: a_T is a unique function of $T - T_g$ for all microstructures in the PB series and also for the noncrystallizable members of the HPB series. This characteristic was used to estimate T_g values for the crystallizable HPB members and gives, by extrapolation, $-70\ °C < T_g \lesssim -105\ °C$ for amorphous polyethylene. The product $J_e°G_N°$ was found to be practically independent of chain microstructure, reflecting the universal nature of the terminal relaxation spectrum for entangled linear polymers with near-monodisperse distributions. The classical form for the modulus shifts, $b_T \propto \rho T$, was shown to be incorrect in general. Variations in both b_T and $G_N°$ with microstructure were analyzed in terms of a recent theory which associates $G_N°$ with the concentration of polymeric Kuhn steps in the liquid.

I. Introduction

A number of important problems in polymer melt rheology have to do with the effects of chain microstructure. Microstructure of course influences a wide range of physical properties—density, melting temperature, glass transition, crystalline morphology, etc. However, both large-scale structure and local structure play important roles in the determination of the rheological properties. Many studies have dealt with the large-scale contribution,[2,3] but comparatively few with the systematic effects of microstructure. The purpose of the present work was to examine the variation in rheological properties of polymer melts with local chain structure. We have used nearly monodisperse systems of linear chains and have focused on those properties which become independent of chain length for long chains, e.g., the temperature coefficients of viscoelastic response, the plateau modulus $G_N°$, and the steady-state recoverable compliance $J_e°$. Two series of samples were used, polybutadienes which had been synthesized with a range of microstructures by anionic polymerization, and fully hydrogenated versions of the same polymers. Depending on polymerization conditions, the polybutadiene (PB) samples range from ~8% to ~99% in vinyl group content. Hydrogenation saturates the backbone double bonds and converts vinyl branches to ethyl branches. The hydrogenated polybutadienes (HPB) are structurally equivalent to copolymers of ethylene and 1-butene with compositions from ~4% to ~99% 1-butene. The proportion of backbone double bonds decreases with increasing vinyl branch frequencies in the PB series; the HPB backbone is of course fully saturated for all ethyl branch frequencies. The effect of long branches will be reported in a later paper on PB and HPB stars.

II. Experimental Procedures

A. Polymerization and Hydrogenation. All samples in this study were prepared by anionic polymerization of butadiene. Conditions were chosen to yield linear chains of high molecular weight ($M > 50\,000$) and narrow molecular weight distribution ($\bar{M}_w/\bar{M}_n < 1.1$). In most cases the polymerizations were conducted at 50 °C in cyclohexane under a nitrogen atmosphere. The capped-bottle technique of Hsieh was used with *sec*-butyllithium as the initiator. The polybutadienyl anions were deactivated with dry 2-propanol stored under nitrogen. Enchainment of butadiene results in three types of structural units–1,4 cis, 1,4 trans, and 1,2 (vinyl). Unmodified polymerization in nonpolar media results in ~8% 1,2 addition. Higher levels of 1,2 addition were obtained by the addition of small quantities of tetrahydrofuran, combined in some cases with a lower polymerization temperature. Samples with nearly 100% 1,2 addition were prepared at the University of Akron by vacuum line techniques. Room-temperature polym-

0024-9297/84/2217-2775$01.50/0

Table I
Chemical Microstructures of Polybutadiene and Hydrogenated Polybutadiene

sample	IR measurements on PB			^{1}H NMR on PB	^{13}C NMR on HPB
	% 1,4 cis	% 1,4 trans	% vinyl	% vinyl	% vinyl
PBV-1.262L	47	45	8.0	8.0	8.4
PBV-1.993L	34	$51._5$	14.5		
PBV-1.015L	33	49	18.0		17.5
PBV-2.124L	29	$51._5$	19.5		
PBV-1.387L	29	48	23.0		23.0
PBV-2.250L	27	$47._5$	25.5		
PBV-1.087L	26	44	30.0		30.8
PBV-2.310L	$23._5$	$41._5$	35.0		
PBV-1.975L	$26._5$	$33._5$	40.0		
PBV-1.042L	20	$37._5$	42.5		
PBV-1.291L	19	30	51.0	49.0	44.0
PBV-1.965L	$16._5$	27	56.5	54.0	53.0
PBV-1.230L	7	$14._5$	78.5		
PBV-1.220L	0	14	86.0		
PBV-0.968L			~100	99	99
PBV-1.927L			~100	99	99
PBV-2.654L			~100	99	99
PBV-3.484L			~100	99	99

Table II
Transition Temperatures of Polybutadiene and Hydrogenated Polybutadiene

sample	polybutadiene		hydrogenated polybutadiene		
	x_{12}	T_g, °C	x_B[b]	T_m, °C	T_x, °C
PBV-1.262L	0.08	−97	0.04_2	111	−30
PBV-1.015L	0.18	−91	0.09_9	91	−40
PBV-1.387L	0.23	−88	0.13_0	75	−45
PBV-1.087L	0.30	−85	0.17_6	72	−51
PBV-1.042L	0.42_5	−73	0.27_0	28	−61
PBV-2.045S[a]	0.46	−70			
PBV-2.255S[a]	0.49	−68			
PBV-1.291L	0.51	−65	0.34_2	−3	−62
PBV-1.965L	0.56_5	−57	0.39_4		−62
PBV-1.890S[a]	0.60	−56			
PBV-2.960L	0.78	−34			
PBV-1.220L	0.86	−25	0.75_5		−42
PBV-0.968L	0.99	−4	0.99		−27
PBV-1.927L	0.99	−5	0.99		−26

[a] Three-arm star polybutadienes. [b] Mole fraction of 1-butene in the equivalent ethylene–1-butene copolymer: $x_B = x_{12}/(2 - x_{12})$.

erization in benzene was used, with *n*-butyllithium as initiator and dipiperidinoethane as modifier. Polymerization procedures and product structures for those polymers are reported elsewhere.[5]

Selected PB samples were hydrogenated to HPB in cyclohexane solution at 75 °C and 700-psi hydrogen pressure with a $Pd/CaCO_3$ catalyst. Procedures are described elsewhere.[6]

B. Chemical Microstructure. The proportion of 1,2 (vinyl), 1,4–cis, and 1,4–trans additions in the butadiene polymerizations were determined by infrared spectroscopy (absorption bands at 910, 735, and 966 cm^{-1}, respectively).[7] Measurements were made with 1–2% PB solutions in carbon disulfide. Molar absorptivities were established with a 99% 1,2-PB (Firestone), a 98% 1,4-*cis*-PB (Goodrich Ameripol CB-220), and a 93% 1,4-*trans*-PB (Phillips Trans-4). The frequency of vinyl groups was also determined by ^{1}H NMR in selected PB samples,[8] and the frequency of ethyl groups was calculated from the concentration of methine carbons (^{13}C NMR) in selected HPB samples.[9] The resulting values of x_{12}, the fraction of 1,2 additions in the butadiene polymerization, are in generally good accord as shown by the summary in Table I. The ratio of cis to trans double bonds in the PB samples remains roughly constant as x_{12} increases.

All samples of HPB were examined for residual unsaturation by infrared spectroscopy (the 10- and 966-cm^{-1} bands), either as films in the case of the partially crystalline samples ($x_{12} < 0.45$ in the parent PB) or as 1–2% solutions in carbon disulfide. Residual unsaturation was also determined for selected HPB samples by ^{13}C NMR in 5–10% trichlorobenzene solutions at 110 °C. No trace of residual double bonds was found for any sample in the present study; levels as high as 0.2% residual unsaturation would have been readily detected.

A more detailed examination of the HPB ^{13}C NMR spectra showed no evidence of other than head-to-tail 1,2 addition. The frequencies of isolated and adjacent 1,2 sequences are essentially random (Bernoullian, with $p = x_{12}$ and $1 - p = x_{14} = 1 - x_{12}$) at low 1,2 content, but there is a definite tendency toward blockiness at the higher levels.[9] The 1,2 sequences in HPB contain a variety of stereoisomeric structures. Those in HPB's made from the 99% vinyl polybutadienes appear to be nearly ideally atactic (Bernoullian with $p = {}^1/_2$),[5] but the proportion of meso and racemic diads for intermediate 1,2 levels was not determined.

We will use x_{12}, the fraction of 1,2 additions in the butadiene polymerization, to designate composition for both the PB and HPB series. the results apply not to all possible PB and HPB microstructures of course but only to the compositional "cuts" represented by these two series of samples.

C. Physical Properties. Glass transition temperatures for the PB samples, determined by differential scanning calorimetry (DSC), are listed in Table II and shown in Figure 1 as a function of vinyl content. Data obtained at both Northwestern University (Perkin-Elmer DSC-2) and the University of Akron (Du Pont-990) are included. Measurements were made at several heating rates, (5, 10, and 20 °C/min), and the temperature at the midpoint of the heat capacity "jump" was extrapolated linearly to zero heating rate. There is no evidence of crystallinity at any vinyl level in this series.

The HPB samples are partially crystalline at the lower 1,2 levels. The final melting temperature, T_m, and the secondary transition temperature, T_x, the latter obtained from the jump in heat capacity at low temperatures, were determined by DSC and are given in Table II.[9] At high 1,2 contents in the PB, the value of T_x clearly corresponds to the glass transition for the noncrystallizing HPB samples. Where crystallinity is present, T_x seems to correspond to the temperature of the β transition as discussed recently by Popli and Mandelkern.[10] The dependence of T_m and T_x on HPB

Table III
Molecular Weight Characterization of Polybutadienes and Hydrogenated Polybutadienes

	polybutadiene					hydrogenated polybutadiene				
sample	x_{12}	$\bar{M}_w$(GPC)	$(\bar{M}_w/\bar{M}_n)_{GPC}$	$\bar{M}_w$(LS)	$\bar{M}_n$(OP)	$\bar{M}_w$(GPC)	$(\bar{M}_w/\bar{M}_n)_{GPC}$	$[\eta]_{THF}$, dL/g	$\bar{M}_w$(LS)	$\bar{M}_w$(calcd)[a]
PBV-1.993L	0.145	165 000	<1.05							171 000
PBV-1.015L	0.18	69 000	<1.05							71 500
PBV-2.124	0.195	175 000	<1.05							181 000
PBV-1.387L	0.23	103 000	<1.05						101 000	106 800
PBV-2.250L	0.255	180 000	<1.05							186 000
PBV-1.087L	0.30	79 000	<1.05						74 100	81 000
PBV-2.310L	0.35	183 000	<1.05							190 000
PBV-1.975L	0.40	168 000	<1.05							174 000
PBV-1.042L	0.42	76 000	<1.05			75 000	<1.05	0.970	78 400	78 900
PBV-1.291L	0.51	104 000	<1.05			102 000	<1.05	1.17	100 400	107 800
PBV-1.965L	0.565	172 000	<1.05			152 000	1.1	1.76		178 000
PBV-1.230L	0.785	121 000	<1.05			156 000	<1.05	1.01		126 000
PBV-1.220L	0.86	110 000	<1.05							114 000
PBV-0.728L	0.99			70 600	65 800		1.05	0.397	73 500	73 200
PBV-0.968L	0.99			106 000	100 000		1.05	0.522	102 000	110 000
PBV-2.654L	0.99			346 000	315 000		1.06	1.346	360 000	359 000
PBV-3.484L	0.99			520 000	480 000		1.10	1.808	526 000	539 000

[a] Calculated from $\bar{M}_w$ of PB (either $\bar{M}_w$(GPC) or $\bar{M}_w$(LS)): M_w(calcd) = (56/54)$(\bar{M}_w)_{PB}$.

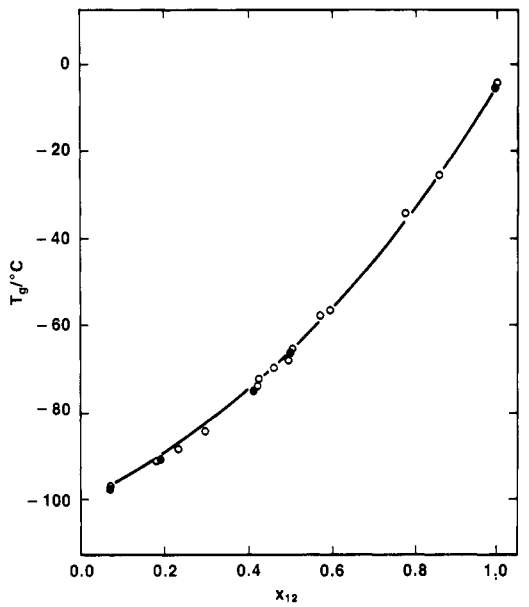

Figure 1. Glass transition temperature vs. composition for polybutadiene. Symbols: (○) measured at Northwestern University; (●) measured at the University of Akron.

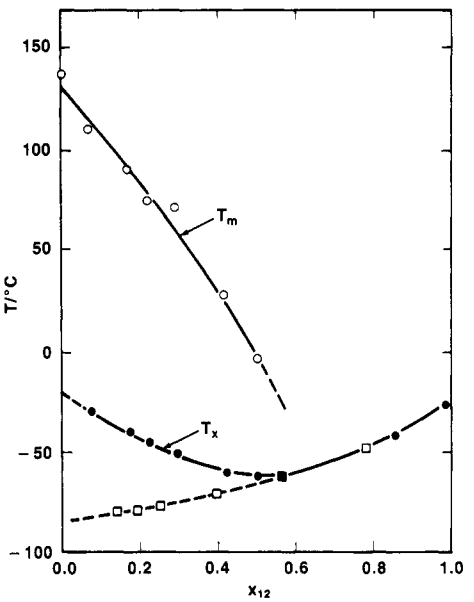

Figure 2. Melting and low-temperature transitions for hydrogenated polybutadiene. Symbols: (○) final melting temperature; (●) transition at low temperature; (□) estimated T_g for the amorphous state, obtained from melt rheology data as described in the text.

composition is shown in Figure 2.

Density was measured at 25 °C for selected samples of PB and HPB in a density gradient column or by a neutral buoyancy method. The values are essentially independent of microstructure for PB: ρ = 0.896 g/cm^3 at low 1,2 levels and 0.890 g/cm^3 at x_{12} = 0.99. Densities of PB's at other temperatures were calculated as needed with an average value of ρ = 0.895 g/cm^3 at 25 °C and a reported value of the thermal expansion coefficient $\alpha = -d \ln \rho/dT = 0.75 \times 10^{-3}$ °C^{-1}.[12] For HPB samples that are noncrystalline at 25 °C ($x_{12} > 0.45$) the density ranges from ρ = 0.860 g/cm^3 (x_{12} = 0.45) to ρ = 0.872 (x_{12} = 0.99) and extrapolates smoothly to 0.855 g/cm^3 at x_{12} = 0, the estimated density of amorphous polyethylene at 25 °C.[11] Judged by data on various olefin homopolymers and copolymers, the melt densities of HPB's at other temperatures probably remain rather close to those for polyethylene melts.[13] Unless otherwise indicated, the densities of HPB melts at elevated temperatures were estimated as required with ρ = 0.806 g/cm^3 at 100 °C and $\alpha = 0.71 \times 10^{-3}$ °C^{-1}.[14]

D. Molecular Weight and Distribution. Average molecular weight and molecular weight distribution breadth for the polybutadiene samples were obtained by a combination of gel permeation chromatography (Waters Associates, Model 200) and on-line intrinsic viscosity measurements in tetrahydrofuran at 25 °C.[15] Universal calibration procedures were used with published values of the Mark–Houwink–Sakurada parameters[5,16] to estimate $\bar{M}_w$ and $\bar{M}_w/\bar{M}_n$ (corrected for axial dispersion in the GPC columns). Values of $\bar{M}_n$ and $\bar{M}_w$ for the 99% vinyl PB's were obtained by membrane osmometry and light scattering.[5]

Molecular weights for the HPB samples were calculated from values for their PB precursors: $M_{HPB} = (56/54)M_{PB}$. Values of $\bar{M}_w$ for selected HPB samples were also obtained by light scattering–GPC measurements at elevated temperatures (trichlorobenzene at 135 °C, dn/dc = −0.104 cm^3/g) through the courtesy of Dr. G. VerStrate, Exxon Chemical Co. For HPB's with x_{12} = 0.99, $\bar{M}_w$ was obtained by light scattering at room temperature (Chromatix KMX-6), and $\bar{M}_w/\bar{M}_n$ was estimated by GPC (Waters Associates Model 150C).[5] Agreement among data obtained by the different methods is reasonably good and supports our earlier conclusion that the large-scale molecular structure is not disrupted during hydrogenation.[6] Results are given in Table III for samples that were selected for the rheological studies on the basis of high molecular weight and narrow distribution.

E. Rheological Measurements. Storage and loss moduli, $G'(\omega)$ and $G''(\omega)$, were measured as functions of frequency (0.001

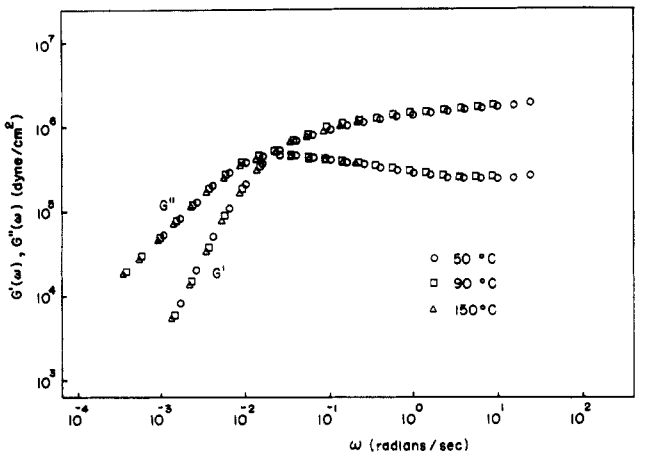

Figure 3. Dynamic moduli for hydrogenated polybutadiene, reduced to 50 °C. The sample is HPB-2.654L (x_{12} = 0.99, $\bar{M}_w$ = 359 000). No shifts in modulus scale were applied.

$< \omega < 100$ s^{-1}) with a Rheometrics mechanical spectrometer, operated in the eccentric rotating disk mode. The values were calculated from steady-state forces and the strain amplitude, corrected for instrumental compliance.[17] Linearity of response was checked repeatedly by measurements of force for different strain amplitudes.

All measurements were made in a nitrogen atmosphere. The PB samples were stabilized with about 0.1% Santonox (Monsanto), the HPB with about 0.1% Irganox 1010 (Ciba-Geigy). Higher stabilization levels were used in some cases for the measurements at elevated temperatures. Thermal stability was checked by repeating measurements at low frequencies after sweeping up through the frequency range. Data were rejected when changes of more than 5% were found. Measurements on several samples were made over as wide a range of temperature as possible. The lowest temperatures was usually room temperature for the PB samples and always above T_m for HPB. The highest temperature was set in most cases by the thermal stability of the sample. Appropriate allowance was made for the change in platen separation distance with temperature. Samples were retrimmed or the platen spacing was adjusted as required at each temperature.

The zero-shear viscosity and steady-state recoverable shear compliance were obtained from the low-frequency response.[3]

$$\eta_0 = \lim_{\omega \to 0} \frac{G''(\omega)}{\omega} \tag{1}$$

$$J_e^\circ = \frac{1}{\eta_0^2} \lim_{\omega \to 0} \frac{G'(\omega)}{\omega^2} \tag{2}$$

Values of η_0 and J_e° are recorded in Tables IV and V.

III. Results and Discussion

A. General Observations. The dynamic moduli of all samples were found to obey the time–temperature superposition principle:[3]

$$G'(\omega,T) = b_T G'(a_T\omega,T_0) \tag{3}$$

$$G''(\omega,T) = b_T G''(a_T\omega,T_0) \tag{4}$$

in which T_0 is a reference temperature and a_T and b_T are shift factors in the frequency and modulus scales for measurements at another temperature T ($a_T = b_T = 1$ at T_0). The modulus shift was very small, as observed in other species: rather good superposition was achievable by shifting only the frequency scale. The example in Figure 3 is typical. Figure 3 also illustrates the general shape of the response curves for all samples in the study. Limiting behavior at low frequencies, $G' \propto \omega^2$ and $G'' \propto \omega$, is succeeded by a crossing of the curves, with $G'(\omega)$ eventually becoming nearly independent of frequency and

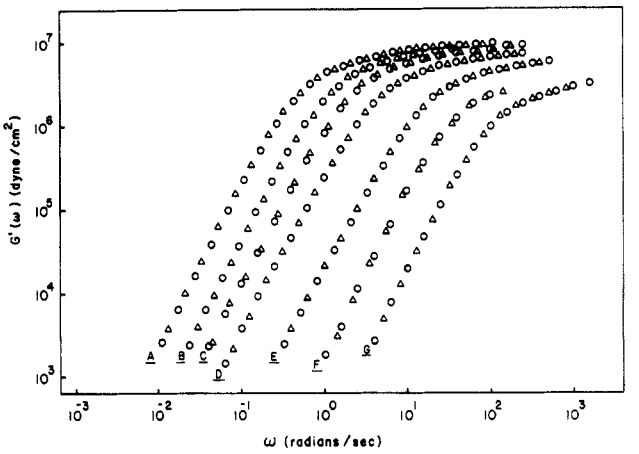

Figure 4. Reduced storage modulus for several polybutadienes. Different reduction temperatures have been used to avoid overlap. Data designations: (A) PB-1.993L ($x_{12} = 0.14_5$), T_0 = 5 °C; (B) PB-2.124L ($x_{12} = 0.19_5$), T_0 = 25 °C; (C) PB-2.250L ($x_{12} = 0.25_5$), T_0 = 50 °C; (D) PB-1.975L (x_{12} = 0.40), T_0 = 75 °C; (E) PB-1.291L (x_{12} = 0.51), T_0 = 70 °C; (F) PB-1.230L ($x_{12} = 0.78_5$), T_0 = 70 °C; (G) PB-0.968L (x_{12} = 0.99), T_0 = 100 °C. No shifts in modulus scale were applied.

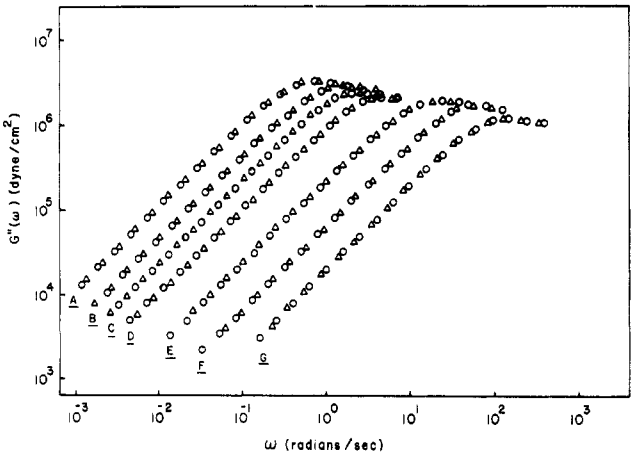

Figure 5. Reduced loss modulus for several polybutadienes. See caption for Figure 4.

$G''(\omega)$ passing through a well-defined maximum G_m'' at ω_m. Such behavior is typical of the terminal and plateau regions for entangled liquids of linear chains with narrow chain length distribution.[18] The transition region lies at still higher frequencies: the onset of that response can be seen rather more clearly in some of the other samples (see Figure 7, for example).

When the terminal and transition responses are resolved, the plateau modulus can be obtained by an integration over the terminal loss peak alone[3]

$$G_N^\circ = \frac{2}{\pi} \int_{-\infty}^{\infty} G''(\omega)\, \mathrm{d} \ln \omega \tag{5}$$

Even when the resolution is incomplete the plateau modulus can be estimated from the terminal loss peak maximum with data for nearly monodisperse linear chains. The relationship

$$G_N^\circ = 3.56 G_m'' \tag{6}$$

has been obtained from an examination of data for several species and chain lengths.[18] Values of G_m'' and the values of G_N° obtained from G_m'' with eq 6 are listed in Tables IV and V.

The effect of chain microstructure on $G'(\omega)$ and $G''(\omega)$ is illustrated in Figures 4 and 5 for several polybutadiene

Table IV
Rheological Properties of Polybutadienes

sample	$\bar{M}_w$	x_{12}	T, °C	η_0, P	$10^7 J_e^0$ cm²/dyn	$10^{-6}G_m''$, dyn/cm²	$10^{-6}G_N^0$, dyn/cm²	$J_e^0 G_N^0$
PBV-1.993L	165 000	0.145	25	3.78×10^6	2.1_8	3.4_0	12.1	2.5
			50	1.27×10^6	2.1_5	3.2_8	11.7	2.5
			75	5.75×10^5	2.2_5	3.3_5	12	2.6
			102	2.98×10^5	2.2	3.3_9	12	2.7
			125	2.03×10^5		3.3_5	12	
PBV-1.015L	69 000	0.18	22	1.64×10^5	2.2	2.9	10.5	2.4
			50	4.31×10^4	2.2	3.1	11.7	2.4
			75	1.82×10^4	1.9	3.1	11.8	2.3
PBV-2.124L	175 000	0.195	25	4.57×10^6	2.3	3.01	10.7	2.4
			50	1.50×10^6	2.4	3.0	10.7	2.5
			75	6.3×10^5	2.4	3.0_5	10.9	2.6
			125	2.1×10^5				
PBV-1.387L	103 000	0.23	25	6.6×10^5	2.3	2.9	10.5	2.5
			50	2.3×10^5	2.3	3.0	11.0	2.5
			75	1.02×10^5		3.0	11.0	
			90	6.64×10^4		3.0	11.0	
PBV-2.250L	180 000	0.255	25	8.4×10^6		2.8_2	10.0	
			50	2.45×10^6	2.4_5	2.9	10.3	2.6
			75	1.00×10^6	2.3_5	2.8_4	10.1	2.5
			100	5.1×10^5	2.3	2.8_3	10.0	2.5
			125	3.0×10^5		2.9	10.3	
PBV-1.087L	79 000	0.30	24	2.35×10^5	2.5	2.6	9.8	2.5
			50	9.1×10^4		2.8	10.0	
			75	3.66×10^4		2.8_5	10.5	
			90	2.4×10^4		2.8_3	10.0	
PBV-2.310L	183 000	0.35	25	8.7×10^6	2.8	2.4_8	8.9	2.5
			50	2.5×10^6		2.6_0	9.2_5	
			75	1.32×10^6	2.9	2.5_5	9.1	2.6
			100	6.24×10^5		2.6	9.3	
			125	4.1×10^5		2.5_5	9.1	
PBV-1.975L	168 000	0.40	25	1.41×10^7		2.45	8.7	
			50	3.23×10^6	2.8	2.5	8.9	2.5
			75	1.1×10^6	2.7	2.5	8.9	2.4
			100	5.2×10^5	2.8	2.4_8	8.8	2.5
			125	3.09×10^5		2.4_8	8.6	
PBV-1.042L	76 000	0.425	24	6.05×10^5	2.6_3	2.4	8.9	2.4
			50	1.56×10^5	2.7_5	2.5	9.3	2.5
			75	5.05×10^4	2.5_5	2.5_5	9.5	2.4
PBV-1.291L	104 000	0.51	24	2.3×10^6		2.1	7.7	
			50	4.84×10^5		2.2	8.1	
			75	1.5×10^5		2.2	8.1	
			95	7.25×10^4		2.2	8.2	
PBV-1.965L	172 000	0.565	25	7.1×10^7		2.0_6	7.3	
			50	1.25×10^7		2.0_6	7.3	
			75	3.5×10^6	3.3	2.0_2	7.2	2.4
			100	1.32×10^6	3.4	1.9_8	7.2	2.5
			125	6.7×10^5		1.9_8	7.1	
PBV-1.230L	121 000	0.785	25	2.95×10^6	3.7_5	1.5_5	5.5	2.1
			50	2.42×10^5	3.9	1.5_8	5.6	2.2
			75	4.21×10^4	3.9	1.5_4	5.5	2.2
			100	1.20×10^4				
PBV-1.220L	110 000	0.86	25	1.22×10^7	4.3	1.3_5	4.8	2.1
			50	5.85×10^5	4.3	1.3_7	4.9	2.2
			75	7.5×10^4	4.3_5	1.3_3	4.7_5	2.1
			100	1.8×10^4				
			126	6.24×10^3				
PBV-0.968L	106 000	0.99	50	2.02×10^6	4.2_6	1.2_6	4.4_8	1.9
			75	1.29×10^5	4.3_6	1.2_1	4.3	1.9
			100	2.10×10^4	4.4	1.2_0	4.2_7	1.9
			125	5.82×10^3				
PBV-2.654L	346 000	0.99	75	1.90×10^7		1.2_6	4.4_5	
			100	2.88×10^6	4.5	1.2_0	4.2_7	1.9
			125	7.69×10^5	4.6	1.1_5	4.1	1.9
			150	2.98×10^5	4.7	1.1_0	3.9	1.9_5
			175	1.46×10^5		1.0_5	3.7_5	
			191	1.12×10^5		0.9_9	3.5_5	

samples. The plateau modulus, i.e., the magnitude of G_m'', decreases progressively with increasing 1,2 content. The curves have the same shape through the terminal region, but the modulus and frequency scales depend on microstructure.

Comparisons of $G'(\omega)$ and $G''(\omega)$ for an HPB and its precursor PB are shown in Figures 6 and 7. The data are plotted in reduced form, $G'(\omega)/G_m''$ and $G''(\omega)/G_m''$ vs. ω/ω_m, to eliminate differences in the modulus and frequency scale factors. In both figures the PB–HPB superposability is excellent at low frequencies ($\omega < \omega_m$), but differences begin to appear at higher frequencies. Figure 6 shows the situation where G_N^0 is virtually the same for PB and HPB ($x_{12} = 0.51$); in this case, PB–HPB super-

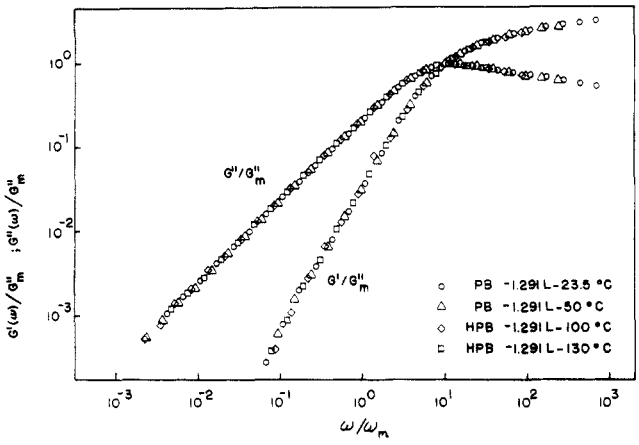

Figure 6. Comparison of reduced dynamic moduli for hydrogenated polybutadiene and its polybutadiene precursor (x_{12} = 0.51).

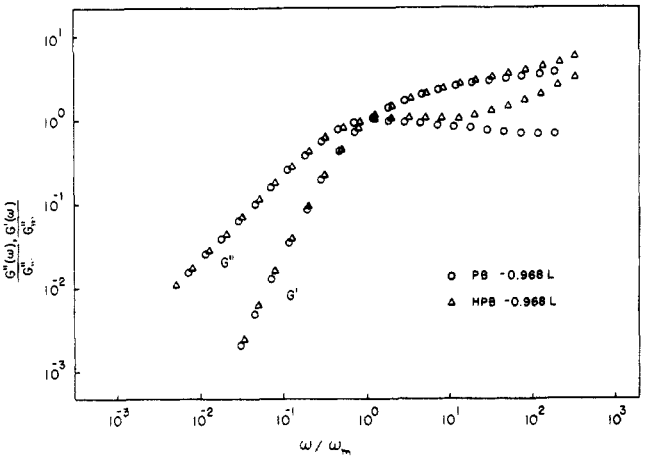

Figure 7. Comparison for reduced dynamic moduli for hydrogenated polybutadiene and its polybutadiene precursor (x_{12} = 0.99).

position is excellent at all frequencies. Figure 7 shows the situation where $G_N°$ is considerably smaller for the HPB (x_{12} = 0.99); here there are substantial departures at higher frequencies.

This general pattern of behavior is understandable simply from the effect of hydrogenation on the plateau modulus. For entangled linear chains the separation between the terminal and transition regions (the plateau width) varies as $(M/M_c)^{3.4}$, where M_c is the characteristic molecular weight for viscosity ($\eta_0 = M^{3.4}$ for $M > M_c$).[3] The entanglement molecular weight

$$M_e = \rho RT/G_N° \tag{7}$$

is closely related to M_c: in many species, $M_c \sim 2M_e$.[2,3] Thus, aside from minor effects due to slight alterations in the molecular weight and density, hydrogenation changes the plateau width by the factor $[(G_N°)_{HPB}/G_N°)_{PB}]^{3.4}$. If $(G_N°)_{HPB}$ is nearly equal to $(G_N°)_{PB}$, as in Figure 6, the terminal–transition separation remains roughly the same, and PB–HPB superposition should remain good even at high frequencies. On the other hand, if $(G_N°)_{HPB}$ is significantly smaller than $(G_N°)_{PB}$, as in Figure 7, the plateau width should decrease with hydrogenation. Contributions from the transition region will thus begin to appear at lower reduced frequencies for the HPB sample, spoiling PB–HPB superposition at high frequencies. Hydrogenation of polybutadiene with low 1,2 content causes a change in the opposite direction; $(G_N°)_{HPB}$ is significantly larger than $(G_N°)_{PB}$, so contributions from the transition region

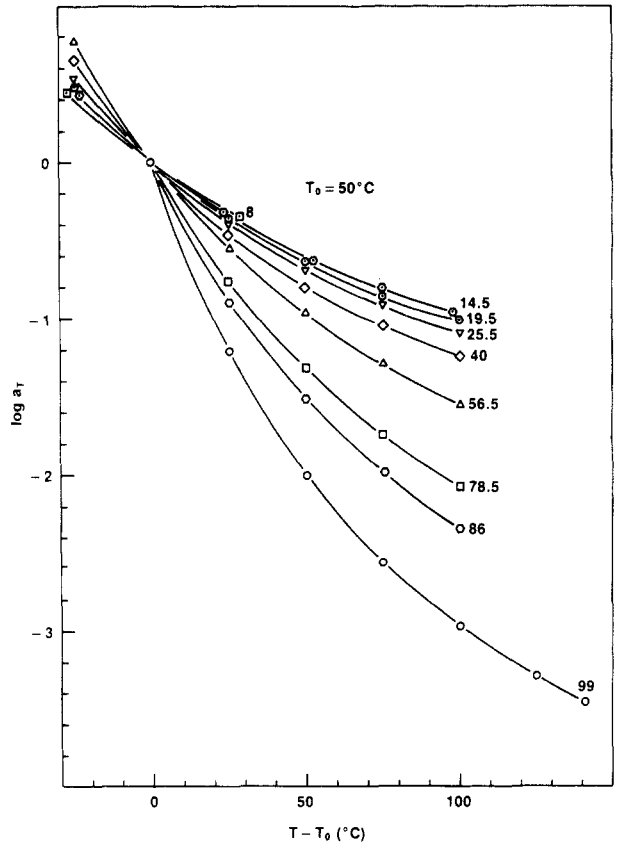

Figure 8. Temperature shift factors for the frequency scale for different polybutadiene microstructures (T_0 = 50 °C).

appear at lower reduced frequencies for the PB samples.

B. Dependence of a_T on Chain Microstructure. If eq 3 and 4 are obeyed, the temperature dependence of all viscoelastic properties depend on a_T and b_T alone. Thus

$$\eta_0(T) = a_T b_T \eta_0(T_0) \tag{8}$$

$$J_e°(T) = J_e°(T_0)/b_T \tag{9}$$

$$G_m''(T) = b_T G_m''(T_0) \tag{10}$$

$$G_N°(T) = b_T G_N°(T_0) \tag{11}$$

In most studies the range of temperatures is simply not wide enough to establish the existence of a shift in modulus scale with temperature. The wide range here, combined with the availability of a well-defined maximum in the terminal loss peak for tracking b_T, makes such measurements possible. Judged by the data on $G_m''(T)$ and $J_e°(T)$ in Tables IV and V, the variation in b_T is certainly weak but still detectable and discernibly different for different microstructures. In some cases it increases slightly with temperature (HPBV-2.654L), in others it remains nearly constant (PBV-2.250L), and in still others it decreases slightly (PBV-2.654L). In no case does it rise as rapidly with temperature as ρT, the classical prediction for the terminal region.[3] This departure from ρT dependence, observed recently for another polymer,[19] will be examined in more detail below.

The variation of b_T in all samples is so slight that, to an excellent approximation, the frequency shift factor a_T can be calculated directly from viscosity data (Tables IV and V):

$$a_T = \eta_0(T)/\eta_0(T_0) \tag{12}$$

Figure 8 shows a_T from eq 12 for polybutadienes of several microstructures for a common reference temperature, T_0

Table V
Rheological Properties of Hydrogenated Polybutadienes

sample	$\bar{M}_w$	x_{12}	T, °C	η_0, P	$10^7 J_e^0$, cm²/dyn	G_m'', dyn/cm²	G_N^0, dyn/cm²	$J_e^0 G_N^0$
HPBV-1.993L	171 000	0.145	110	1.54×10^6	1.2_6	5.9	21	2.6
			130	8.61×10^5		5.8	20.5	
			160.5	4.12×10^5	1.3	5.8	20.5	2.6
			190.5	2.4×10^5	1.2_8	5.7_5	20.5	2.6
			220	1.53×10^5	1.3	5.7	21	2.6
HPBV-1.015L	71 500	0.180	130	2.7×10^4		5.5	18.2	
			190	8.2×10^3				
HPBV-2.124L	181 000	0.195	110	1.75×10^6	1.3_6	5.3	18.9	2.6
			130	9.55×10^5	1.3_8	5.2	18.5	2.5
			160.5	4.46×10^5	1.3_8	5.0	18.0	2.5
			190	2.57×10^5	1.3_8	5.1	18.1	2.5
			220	1.64×10^5		5.0	17.8	
HPBV-1.387L	107 000	0.23	130	1.4×10^5		5.0_5	16.2	
			190	4.26×10^4				
HPBV-2.250L	186 000	0.255	110	2.54×10^6		4.6	16.5	
			130	1.35×10^6		4.4	15.8	
			160	6.61×10^5		4.5	16.0	
			190	3.78×10^5	1.7	4.3	15.5	2.6
			220	2.54×10^5		4.2_5	14.8	
HPBV-1.087L	82 000	0.30	130	4.6×10^4		4.2	13.6	
			190	1.25×10^4		4.3	13.9	
HPBV-2.310L	190 000	0.35	130	1.78×10^6		3.5_5	12.7	
			160	7.0×10^5		3.5	12.5	
			190.5	3.63×10^5	2.1	3.5	12.5	2.6
			219.5	2.4×10^5		3.4_5	12.3	
HPBV-1.975L	174 000	0.40	110	1.51×10^6		3.1_5	11.2	
			130.5	8.03×10^5		3.2_5	11.6	
			160.5	3.59×10^5	2.4_5	3.1	11.0	2.7
			190.5	1.90×10^5		3.0	10.7	
			220	1.15×10^5				
HPBV-1.042L	79 000	0.425	130	4.0×10^4	2.4_5	3.4	10.9	2.6
			190	1.0×10^4		3.4_5	11.0	
HPBV-1.291L	108 000	0.51	100	2.24×10^5		2.6	8.6	
			130	8.1×10^4		2.6		
HPBV-1.965L	178 000	0.565	74.5	1.42×10^7	3.3_8	2.3_5	8.3_5	2.8
			99.5	4.42×10^6		2.3_5	8.3_5	
			125.5	1.68×10^6	3.4	2.2_8	8.1	2.7
			150.5	7.94×10^5		2.2	7.9	
			175	4.38×10^5		2.1_5	7.7	
			200	2.61×10^5		2.1	7.5	
HPBV-1.230L	126 000	0.785	25	4.09×10^6	4.6	1.2_2	4.3_5	2.0
			50.5	3.21×10^5	4.6	1.2_3	4.3_8	2.1
			75	5.37×10^4	4.6	1.2_0	4.2	2.0
			100	1.39×10^4	4.5	1.1_8	4.2_7	1.9
HPBV-0.728L	73 000	0.99	26	9.15×10^5	1.0_6	0.53	1.9_0	2.0
			50	5.01×10^4	1.0_8	0.54_5	1.9_2	1.9
HPBV-0.968L	109 000	0.99	30	1.97×10^6	$10._9$	0.53	1.8_9	2.0
			50	2.02×10^5	$11._3$	0.54	1.9_4	2.2
			75	2.43×10^4	$10._6$	0.56	1.9_9	2.1
			100	5.01×10^3	$10._4$	0.56	1.9_8	2.0
HPBV-2.654L	360 000	0.99	50	4.57×10^7	11	0.49_5	1.7_5	1.9
			75	5.25×10^6	11	0.51	1.8_0	2.0
			100	1.09×10^6	11	0.52	1.8_5	2.0
			125	3.03×10^5	$10._5$	0.53_5	1.9_0	2.0
			150	1.15×10^5	$10._5$	0.55	1.9_5	2.1
			170	6.31×10^4	10	0.56	2.0_0	2.0
			190	3.63×10^4	10	0.56	2.0	2.0
			210	2.26×10^4	10	0.56_5	2.0	2.0
HPBV-3.484L	539 000	0.99	75	2.29×10^7	$10._6$	0.52_5	1.9	2.0
			100	4.36×10^6	$10._0$	0.54_3	1.9	1.9

= 50 °C. The variation with composition is obviously quite large and, as it turns out, mainly related to the variation in glass transition temperature with chain microstructure. The frequency shift is well described by a WLF equation:[3]

$$\log a_T = \frac{A(T - T_0)}{B + (T - T_0)} \tag{13}$$

The curves in Figure 8 were calculated from eq 13 with values of A and B obtained empirically for each microstructure.[20]

As found earlier by Kraus and Gruver,[21] all the PB data can be represented as a single curve by locating T_0 for each composition at a constant distance from T_g. Figure 9 shows the result for $T_0 = 55$ °C + T_g (corresponding to $T_0 = 50$ °C for $x_{12} = 0.99$). The line in the figure was calculated from

$$\log a_T = \frac{5.78(T - T_g - 55)}{94.8 + (T - T_g - 55)} \tag{14}$$

Equation 14 applies in the experimental temperature range of 100–200 °C above T_g for the low-vinyl compositions and from 50–150 °C above T_g for high-vinyl compositions. A single pair of WLF coefficients and the location of T_g alone govern the temperature dependence of viscoelastic re-

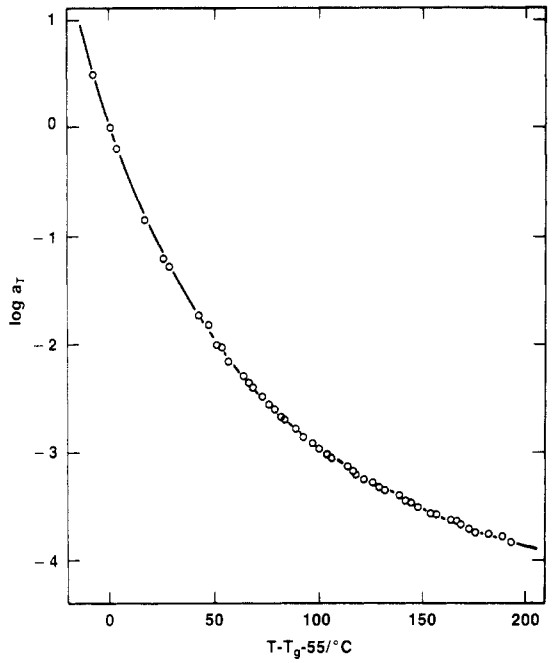

Figure 9. General correlation of temperature shift factors for the frequency scale in polybutadienes of all microstructures.

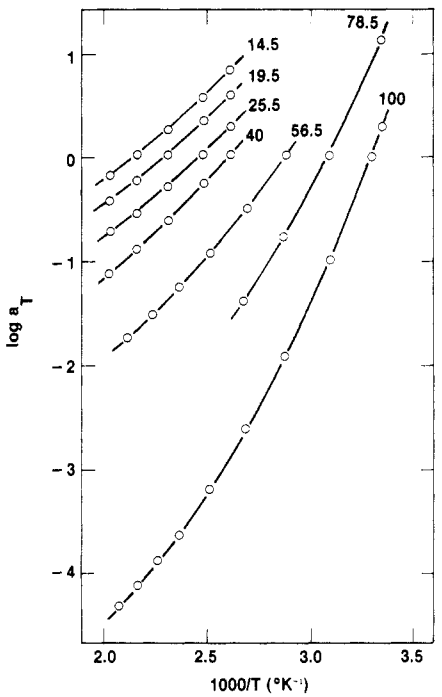

Figure 10. Temperature shift factors for the frequency scale for different microstructures of hydrogenated polybutadiene. The curves have been displaced vertically to avoid overlap.

sponse for the entire range of polybutadiene microstructures: the temperature coefficient of viscosity is a function of $T - T_g$ alone. The similar reductions for polyisoprene and for hydrogenated polyisoprene cover somewhat narrower ranges of microstructure.[19] Of course, the WLF coefficients for constant $T_0 - T_g$ are not universal,[3] but they are quite insensitive to microstructure over some range of compositions and temperatures, and that range can apparently be quite large in some cases.

The temperature shifts for HPB melts of various microstructures are shown in Figure 10. The results agree well with similar data on HPB samples published earlier by Arnett and Thomas.[22] The available range of temperatures at small x_{12} is somewhat restricted in this series

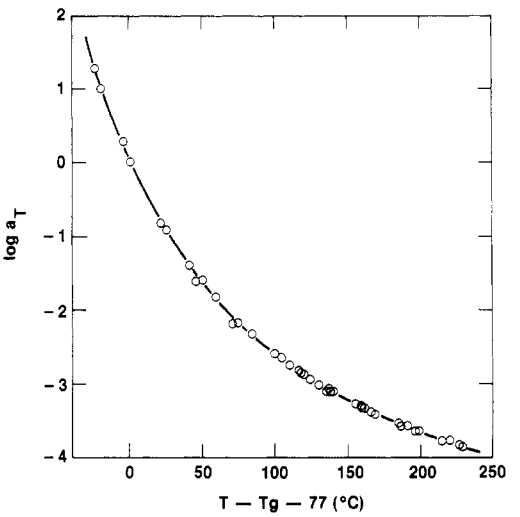

Figure 11. Generalized correlation of temperature shift factors for the frequency scale in hydrogenated polybutadienes of all microstructures. The values of T_g for the crystallizable compositions were chosen as described in the text.

Table VI
Rheological Estimates of Glass Transition Temperatures for Hydrogenated Polybutadiene Melts

sample	x_{12}	T_g
HPB-1.993L	0.145	−80
HPB-2.124L	0.195	−79
HPB-2.250L	0.255	−77
HPB-1.975L	0.40	−71
HPB-1.965L	0.565	−62
HPB-1.230L	0.785	−48
HPB-2.654L	0.99	−27

by crystallization. The data are plotted according to the Arrhenius form (log a_T vs. $1/T$); different reference temperatures were used for each microstructure to avoid crowding. Despite the very high temperatures relative to T_g (up to T_g + 270 °C for x_{12} = 0.565 and T_g + 240 °C for x_{12} = 0.99), the plots remain curved. There is no clearly defined Arrhenius region at high temperature, corresponding to a constant flow activation energy $E_v \equiv R\ \mathrm{d}\ \ln \eta_0/\mathrm{d}T^{-1}$. The data are, in fact, well correlated by the WLF form (eq 13) even at the highest temperatures: the WLF fits are shown as lines in Figure 10.

The change in temperature dependence with HPB microstructures is qualitatively similar to that for the PB series, suggesting the possibility of a similar unified form. Because of crystallinity, however, unambiguous glass transition temperatures for HPB are available only for $x_{12} > 0.55$. The value of T_g for crystallizable polymers is, in fact, a matter of some debate,[10,22-24] and particularly so for linear polyethylene, corresponding to the $x_{12} = 0$ limit in the HPB series. We estimated values for T_g for the crystallizable HPB compositions in the following manner. First, we assumed that a unified expression for a_T of the same form as eq 14 applies in the melt state for the entire HPB series. Next, we established the coefficients of that equation with data for the noncrystallizing samples of HPB ($nx_{12} > 0.55$) using their calorimetrically determined T_g values and T_0 = 77 °C + T_g (corresponding to T_0 = 50 °C for x_{12} = 0.99) in those cases. Finally, we searched for values of T_g for the crystallizable compositions ($x_{12} < 0.55$) that would produce a fit to this same expression. The resulting unified curve is shown in Figure 11; the line in the figure was calculated from

$$\log a_T = \frac{6.35(T - T_g - 77)}{146 + (T - T_g - 77)} \qquad (15)$$

Values of T_g estimated for the crystallizable samples by the requirement of unification are given in Table VI and plotted in Figure 2.

There is some latitude for the choice of these T_g values, particularly at low x_{12}, where the extrapolation is rather long, but it is clear that T_g for the HPB series, as seen from the melt state, decreases monotonically with decreasing ethyl branch content. It certainly does not track T_x at low x_{12} levels, thus ruling out the sometimes suggested value of $T_g \sim -30$ °C for amorphous linear polyethylene ($x_{12} = 0$). Another suggested value, $T_g \sim -120$ °C, is somewhat lower than the "rheological" estimate, $-70 > T_g \gtrsim -105$ °C, but it cannot be entirely ruled out. The average value of $T_g = -85$ °C is similar to estimates for amorphous polyethylene obtained by other methods.[24,25]

C. Dependence of J_e° and G_N° on Chain Microstructure. Beyond a characteristic molecular weight $M_c' \sim 6M_e$, the steady-state recoverable compliance is independent of molecular weight for linear chains with narrow distribution.[2] The molecular weight of all samples in this study are much larger than $6M_e$, so J_e°, like G_N°, should be a function of the microstructure alone. Values of $J_e^\circ G_N^\circ$ are given in Tables IV and V for the two series of microstructures. Except for the PB's and HPB's at $x_{12} = 0.99$, the product $J_e^\circ G_N^\circ$ ranges only from 2.4 to 2.7, a span that corresponds roughly with the experimental error in the measuring of G_m'' and J_e° for different samples. The magnitude of $J_e^\circ G_N^\circ$ depends on the breadth of the terminal relaxation spectrum.[12] Constancy with microstructure is simply further confirmation of the universal form of the terminal spectrum for highly entangled liquids of nearly monodisperse linear chains.[18] The somewhat smaller values of $J_e^\circ G_N^\circ$ for the high-vinyl PB's and derived HPB's may well reflect slightly narrow chain length distributions in those samples.

Individually, G_N° and J_e° are expected to be functions of the chain microstructure. It has been suggested that the plateau modulus is a universal function of the total length of chain per unit volume, measured in units of the Kuhn step length for the species.[26] The proposed form is a power law

$$G_N^\circ l^3/kT = K(\nu L l^2)^d \tag{16}$$

in which L is the contour length per chain, ν is the number of chains per unit volume, K is a universal constant, and l is the Kuhn step length. As defined by Flory,[27] $l = C_\infty l_0$, in which C_∞ is the characteristic ratio of the species, and l_0 is the average skeletal bond length. Since $\nu = N_A\rho/M$ for melts (N_A is Avogadro's number), the total length of chain per unit volume is $N_A\rho l_0/m_0$, m_0 being the average molecular weight per skeletal bond. The average bond length is constant in the HPB series; it increases slightly with x_{12} in the PB series because the proportion of internal double bonds decreases, but that effect is small. For isothermal comparisons within a series of compositions having about the same melt density and skeletal bond length

$$G_N^\circ \propto m_0^{-d} C_\infty^{2d-3} \tag{17}$$

The exponent $d \sim 2.3$ was deduced from the concentration dependence of G_N° for both 8% vinyl PB[26] and the derived HPB.[18] We will assume this value applies for all PB and HPB microstructures. Values of C_∞ have been measured for several microstructures in the two series and are listed in Table VII.

Figure 12 shows plateau modulus at $T \sim 100$ °C as a function of composition for the two series. In both PB and HPB the value of G_N° decreases with increasing 1,2 content, and the decrease is more rapid in the HPB series.

Table VII
Values of Characteristic Ratio and Plateau Modulus[a]

polymer	x_{12}	m_0	C_∞	G_N^0, dyn/cm^2
polybutadiene	0.08	14.1	5.1 (26.5 °C)[36]	1.25×10^7
polybutadiene	0.43	17.2	6.1 (15.7 °C)[37]	9.3×10^6
polybutadiene	0.99	26.7	7.0 (32.8 °C)[5]	4.2×10^6
polyethylene	0.00	14.0	7.2 (100 °C)[27]	$2.7 \times 10^{7\,b}$
hydrogenated polybutadiene	0.43	17.8	6.4 (65.0 °C)[37]	1.1×10^7
hydrogenated polybutadiene	0.99	27.7	5.5 (100 °C)[5]	1.9×10^6

[a] All values of C_∞ are based on intrinsic viscosity data at Θ conditions with the Fox–Flory constant $\Phi = 2.5 \times 10^{21}$. The value for polyethylene at 140 °C was converted to 100 °C with the temperature coefficient of chain dimensions $\kappa = d \ln C_\infty/dT = -1.1 \times 10^{-3}$ °C^{-1}.[27] The value for HPB at $x_{12} = 0.99$ was converted from 5.3 at 23.5 °C[5] to 100 °C with $\kappa = 0.5 \times 10^{-3}$ °C^{-1} for atactic poly(1-butene).[27] Values of κ are not available for the other compositions; we assume the corrections of C_∞ to 100 °C are negligible. We have not used values reported by Stacy and Arnett[38] for several HPB compositions, based on non-Θ measurements, although their results are in general accord with the values given above. [b] Estimated from Figure 12 as G_N^0 for HPB extrapolated to $x_{12} = 0$.

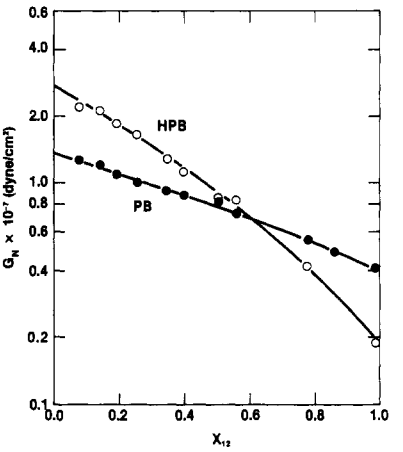

Figure 12. Plateau modulus vs. microstructure for polybutadiene and hydrogenated polybutadienes.

Each of these observations is qualitatively consistent with eq 17. The values of m_0 for each composition are given by

$$m_0 = 27/(2 - x_{12}) \quad \text{PB series} \tag{18}$$

$$m_0 = 28/(2 - x_{12}) \quad \text{HPB series} \tag{19}$$

They increase with 1,2 content in both series, driving G_N° down as $m_0^{-2.3}$. The values of C_∞ increase with vinyl content in th PB series, driving G_N° up as $C_\infty^{1.6}$ and tending to offset the effect of increasing m_0. The values of C_∞ decrease with increasing ethyl branch content in the HPB series, in this case accentuating the effect of increasing m_0.

Even the quantitative predictions of eq 17 are reasonable in most cases. Thus, G_N° decreases by the factor $0.42/1.25 = 0.34$ in going from $x_{12} = 0.08$ to $x_{12} = 0.99$ in the PB series, and eq 17 predicts 0.38. Hydrogenation reduces G_N° by the factor $1.9/4.2 = 0.45$ for $x_{12} = 0.99$, and eq 17 predicts 0.62. Hydrogenation increases G_N° by the factor $1.1/0.92 = 1.18$ for $x_{12} = 0.43$, and eq 17 predicts 1.00. However, the change with composition across the HPB series is somewhat larger than predicted: from $x_{12} = 0.08$ to $x_{12} = 0.99$, G_N° decreases by the factor $0.19/2.7 = 0.070$, but eq 17 predicts 0.135.

More detailed examination of the HBP results at small and intermediate values of x_{12} shows a pattern of departures from the simple proportionality suggested by eq 17.

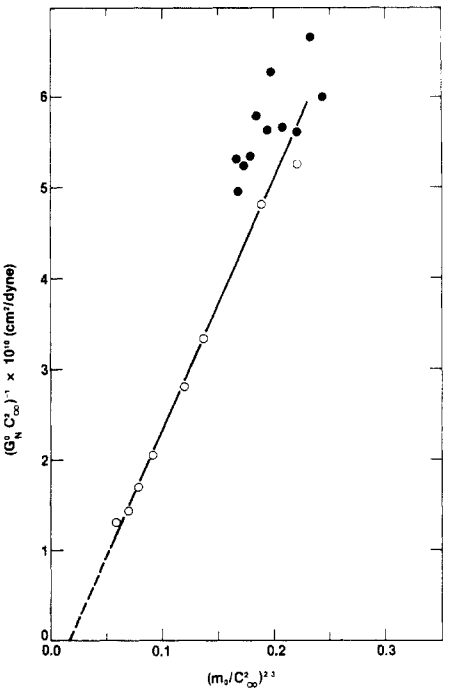

Figure 13. Plateau modulus vs. chain properties as suggested by eq 20–22 of the text. Symbols: (●) polybutadienes; (○) hydrogenated polybutadienes. The line was used to determine the numerical coefficients in eq 23.

The behavior in fact seems more consistent with a modified form of eq 16:

$$(G_N^\circ l^3/kT)^{-1} = K_1(\nu L l^2)^{-2.3} - K_2 \tag{20}$$

reducing to eq 16 for $K_2 = 0$. The dimensionless plateau modulus and contour length concentration can be written

$$G_N^\circ l^3/kT = (N_A l_0^3/kT) G_N^\circ C_\infty^3 \tag{21}$$

and

$$\nu L l^2 = (\rho N_A l_0^3) C_\infty^2/m_0 \tag{22}$$

Equation 20 can thus be tested for the HPB series by a plot of $(G_N^\circ C_\infty^3)^{-1}$ vs. $(m_0/C_\infty^2)^{2.3}$. Values of C_∞ for HPB's at intermediate compositions were interpolated from the C_∞ data in Table VII. Values of m_0 were calculated from eq 19. The results for $x_{12} < 0.6$ are shown in Figure 13. Results obtained similarly for the PB series are included for comparison.

The HPB data lie along a straight line, but with a nonzero intercept ($K_2 \neq 0$). The PB data, on the other hand, merely reduce to a cluster of points: the contour length concentration $\nu L l^2$ does not change significantly across the PB series. A positive value of K_2 implies that the plateau modulus becomes infinite at some finite value of contour length concentration. The line drawn in Figure 13 translates to the following dimensionless equation:

$$(G_N^\circ l^3/kT)^{-1} = 136[(\nu L l^2)^{-2.3} - (10.0)^{-2.3}] \tag{23}$$

Accordingly, the plateau compliance $J_N^\circ \equiv (G_N^\circ)^{-1}$ extrapolates to zero at a finite value of the reduced contour length concentration:

$$(\nu L l^2)_{crit} = 10.0 \tag{24}$$

This result, of course, must be viewed with some caution. The intercept in Figure 13 is small and obtained by a relatively long extrapolation. Interpolations to estimate C_∞ at intermediate compositions can also be hazardous. On the other hand, based on current interpretations of the plateau region, it is not unreasonable to except some complication at sufficient large contour length concentrations. The magnitude of G_N° is assumed to reflect a certain distance scale along the chains, set by the constraint of mutual uncrossability. The chains are free to flex and relax locally: chain segments up to that length scale behave roughly as they would in a rubber network. Accordingly, a liquid of sufficiently long chains should act at intermediate times like a network of Gaussian strands if the length scale is large compared to the Kuhn step. From eq 16, the length scale decreases with increasing concentration of contour length, giving a higher concentration of "strands" and a correspondingly larger modulus. However, as that entanglement length scale begins to approach the Kuhn step length the laws governing mechanical response should certainly change, perhaps becoming more like those for a densely locked collection of locally ordered, semiflexible rods.[28]

The modulus would not, of course, become literally infinite as this "critical" contour length concentration is approached, but it could easily rise by a few orders of magnitude, making G_N° very large compared with the modulus of the corresponding Gaussian network. Equation 20 implies a simple additivity of compliances for those two components of the response. Ronca has also mentioned the possibility of a critical length ratio in a recent discussion of entangled chain dynamics.[31]

How generally applicable are the numerical coefficients in eq 23? That equation, like eq 16, provides an approximate fit of data for many species, but in most all cases the effect of the second term is too small to make much difference. Undiluted polyethylene ($x_{12} = 0$) has an unusually large contour length concentration, $(\nu L l^2)_{PE} = 6.6$, although still somewhat smaller than the apparent critical value of about 10. There are polymers with a larger plateau modulus than polyethylene,[32] but characteristic ratios are not available.

A size scale associated with entanglement can be obtained from the plateau modulus with the Doi–Edwards molecular theory.[33] In the terms used here[34]

$$G_N^\circ = {}^4/_5(\nu L l kT/a^2) \tag{25}$$

where a is the step length associated with the "tube" that confines each chain in a melt of chains. This equation should apply to the network-like contribution to the modulus, given by eq 23 when the second term is set to zero:

$$G_N^\circ l^3/kT = {}^1/_{136}(\nu L l^2)^{2.3} \tag{26}$$

When the Doi–Edwards expression is substituted for G_N° in eq 26

$$a/l = 10.4/(\nu L l^2)^{0.65} \tag{27}$$

Accordingly, at the critical contour length concentration (eq 24)

$$(a/l)_{crit} = 2.3 \tag{28}$$

Thus, the numerical quantities are not unreasonable: flexible chain response is lost as the step length of the tube approaches the Kuhn step length of the chain. For polyethylene melts the ratio (from eq 27) is only slightly larger than the critical value

$$a/l \sim 3.1 \tag{29}$$

The ratio is larger for HPB at $x_{12} = 0.99$

$$a/l \sim 7.2 \tag{30}$$

and for the entire PB series

$$a/l \sim 4.3 \tag{31}$$

D. Temperature Dependence of the Plateau Modulus. We observed earlier that the modulus shift factor

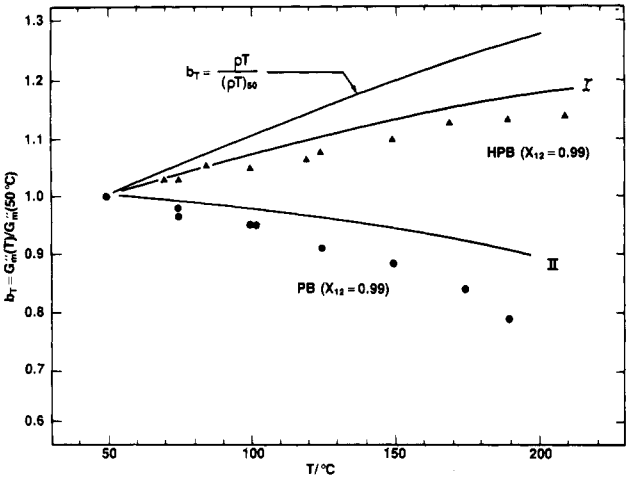

Figure 14. Temperature shift factors for the modulus scale in high-vinyl polybutadiene and hydrogenated polybutadiene. Symbols: (●) PB, x_{12} = 0.99; (▲) HPB, x_{12} = 0.99. Line I was calculated with eq 32 using reported data for atactic polybutadiene; line II was also calculated with eq 32 (see text).

b_T is a weak function of temperature and that the dependence varies with the chain microstructure. It is usual to assume that b_T in the plateau and terminal regions varies universally as ρT, an expectation based on the Rouse model.[3] Equation 16, on the other hand, suggests a different temperature dependence, and one which varies with the polymer species.[26] Thus, since $G_N°(T) \propto b_T$ (eq 11), we can pick out the terms in eq 16 that depend on temperature to obtain

$$b_T = \frac{G_N°(T)}{G_N°(T_0)} = \frac{\rho^d T C_\infty^{2d-3}}{[\rho^d T C_\infty^{2d-3}]_0} \tag{32}$$

where d = 2.3.

Values of b_T were calculated from the $G_m''(T)$ data in Tables IV and V using eq 10 and T_0 = 50 °C. The results are shown in Figure 14 for two microstructures, PB at x_{12} = 0.99 and HPB at x_{12} = 0.99. The Rouse model form

$$b_T = \rho T/(\rho T)_0 \tag{33}$$

which differs negligibly for the two microstructures, is also shown in Figure 14. Line I in Figure 14 was calculated from eq 32 for the HPB sample with known values for atactic poly(1-butene): $\kappa = \mathrm{d} \ln C_\infty/\mathrm{d}T = 0.50 \times 10^{-3}$ °C^{-1} [27] and $\alpha = -\mathrm{d} \ln \rho/\mathrm{d}T = 0.91 \times 10^{-3}$ °C^{-1}.[35] Allowing for some uncertainity in κ, the agreement of eq 32 with the experimental result is rather good, certainly much better than the Rouse form. The behavior of b_T for hydrogenated polyisoprene, where values of α and κ are also available, supports eq 32[19] and disagrees with the clasical ρT dependence.

The temperature coefficient of chain dimensions is not known for high-vinyl PB. Line II was calculated from eq 32 with $\alpha = 0.71 \times 10^{-3}$ °C^{-1} for PB and an arbitrary choice of $\kappa = -0.40 \times 10^{-3}$ °C^{-1}. A value in the range $\kappa \sim -1 \times 10^{-3}$ °C^{-1} would be required to fit the data. The Rouse form (eq 33) is obviously unsatisfactory. Ronca's expression for plateau modulus[31] suggests a still different form for the modulus shift, $b_T \propto T\rho^3 C_\infty^3$, which cannot be distinguished from eq 32 within the error limits of the data.

Although b_T is a weak function of temperature in any case, the results established here are not without interest. They suggest that the ρT adjustment should not be applied routinely to viscoelastic measurements in the plateau and terminal regions. No shift at all would be more appropriate in many instances. The apparent involvement of $C_\infty(T)$ with b_T also suggests a connection between the modulus shift for a polymer species and the temperature coefficient of viscosity for branched chains with the same microstructure. According to a recent analysis,[39] polymers with long branches and $\kappa < 0$ are expected to show an enhanced temperature coefficient of viscosity and thermorheological complexity, i.e., violation of time–temperature superposition. The validity of this inference will be examined in a forthcoming paper on PB and HPB stars.

IV. Summary and Conclusions

The effect of chain microstructure on viscoelastic properties has been investigated for two series of linear polymers, polubutadienes with vinyl content from 8% to 99% ($0.08 < x_{12} < 0.99$) and their fully hydrogenated counterparts. The PB samples are amorphous at all temperatures, T_g increasing from −97 to −4 °C with vinyl content. Hydrogenation was accomplished without disruption of the large-scale structure and yields HPB products that are equivalent in microstructure to copolymers of ethylene and 1-butene. Below x_{12} = 0.45 the HPB's are partially crystalline at 25 °C, with melting temperatures ranging up to 111 °C at x_{12} = 0.08. All samples have narrow molecular weight distributions ($\bar{M}_w/\bar{M}_n < 1.1$) and high enough molecular weights to lie well within the entanglement region.

Dynamic moduli were measured for the melts over an unusually wide range of temperatures. The time–temperature superposition principle was obeyed in all cases; shifts in frequency scale conformed to the WLF equation. In the PB series the temperature coefficient was a unique function of $T - T_g$: a single set of WLF constants correlate a_T for all PB composition when the reference temperature for each was chosen at a constant interval above the glass transition. A similar consolidation of microstructural effects was assumed to occur in HPB melts and then used as an extrapolation device to locate glass transitions for the crystallizable compositions. For amorphous polyethylene (x_{12} = 0), $-105 \lesssim T_g < -70$ °C was obtained.

A very weak but still measurable dependence on temperature was found for the modulus shift factor b_T. The results were clearly inconsistent with the Rouse form, $b_T \propto \rho T$, but in reasonable accord with $b_T \propto \rho^d T C_\infty^{2d-3}$ (d = 2.3), a form suggested in a recent theoretical discussion of the plateau modulus.

The variation of $G_N°$ with chain microstructure was examined for both the PB and HPB series. The dependence on x_{12} in the PB series was roughly consistent with the proposal that $G_N°$ is a universal function of the concentration of chain contour, measured in units of the Kuhn length. The HPB series extends to unusually large values of this concentration at small x_{12}; the results there suggest the existence of a critical contour length concentration, beyond which the Gaussian network character of the entanglement plateau is replaced by a much stiffer response.

Acknowledgment. This work was supported by the National Science Foundation (Grant CPE80-00030), the Northwestern University Materials Research Center (Grant DMR79-23573), and the National Research Council of Argentina (CONICET). We are grateful to Dr. M. J. Struglinski for NMR measurements, to Dr. G. VerStrate of Exxon Chemical Co. from molecular weight measurements and valuable discussions, and to Dr. J. T. Gotro for help with many phases of the work.

References and Notes

(1) Present address: (a) PLAPIQUI, 8000 Bahia Blanca, Argentina. (b) Corporate Research Science Laboratories, Exxon Research and Engineering Co., Clinton Township, Annandale, NJ 08801.

(2) W. W. Graessley, *Adv. Polym. Sci.*, **16**, 1 (1974).
(3) J. D. Ferry, "Viscoelastic Properties of Polymers", 3rd ed., Wiley, New York, 1980.
(4) H. L. Hsieh, *J. Polym. Sci., Part A*, **3**, 153 (1965).
(5) Z. Xu, N. Hadjichristidis, J. M. Carella, and L. J. Fetters, *Macromolecules*, **16**, 925 (1983).
(6) H. Rachapudy, G. G. Smith, V. R. Raju, and W. W. Graessley, *J. Polym. Sci., Polym. Phys. Ed.*, **17**, 1211 (1979).
(7) R. S. Silas, J. Yates, and V. Thornton, *Anal. Chem.*, **31**, 529 (1959).
(8) Y. Tanaka, Y. Takeuchi, and M. Tadakoro, *J. Polym. Sci., A-2*, **9**, 43 (1971).
(9) T. M. Krigas, J. M. Carella, M. J. Struglinski, F. C. Schilling, B. Crist, and W. W. Graessley, manuscript in preparation.
(10) R. Popli and L. Mandelkern, *Polym. Bull.*, **9**, 260 (1983).
(11) J. Brandrup and E. H. Immergut, Eds., "Polymer Handbook", Wiley, New York, 1975.
(12) J. F. Saunders, R. H. Valentine, and J. D. Ferry, *J. Polym. Sci., Part A-2*, **6**, 967 (1965).
(13) D. W. Van Krevelen, "Properties of Polymers", 2nd ed., Elsevier, Amsterdam, 1976.
(14) M. J. Richardson, P. J. Flory, and J. B. Jackson, *Polymer*, **4**, 221 (1963).
(15) W. S. Park and W. W. Graessley, *J. Polym. Sci., Polym. Phys. Eds.*, **15**, 85 (1977).
(16) G. Kraus and C. J. Stacy, *J. Polym. Sci., Part A-2*, **10**, 657 (1972).
(17) V. R. Raju, G. G. Smith, G. Marin, J. R. Knox, and W. W. Graessley, *J. Polym. Sci., Polym. Phys. Ed.*, **17**, 1183 (1979).
(18) V. R. Raju, E. V. Menezes, G. Marin, W. W. Graessley, and L. J. Fetters, *Macromolecules*, **14**, 1668 (1981).
(19) J. T. Gotro and W. W. Graessley, *Macromolecules*, preceding paper in this issue.
(20) J. M. Carella, Doctoral Thesis, Northwestern University, 1983.
(21) G. Kraus and J. T. Gruver, *Rubber Chem. Technol.*, **42**, 800 (1969).
(22) R. L. Arnett and C. P. Thomas, *J. Phys. Chem.*, **84**, 649 (1980).
(23) F. C. Stehling and L. Mandelkern, *Macromolecules*, **3**, 242 (1970); R. F. Boyer, *Macromolecules*, **6**, 288 (1973).
(24) R. Lam and P. Geil, *J. Macromol. Sci., Phys.*, **B20**, 37 (1981).
(25) J. J. Maurer, *Rubber Chem. Technol.*, **38**, 979 (1965).
(26) W. W. Graessley and S. F. Edwards, *Polymer*, **22**, 1329 (1981).
(27) P. J. Flory, "Statistical Mechanics of Chain Molecules", Wiley-Intersciences, New York, 1969.
(28) It is perhaps worth noting that $\nu L l^2 = 10$ is still well below the range required for liquid crystalline ordering of Kuhn steps in the undiluted polymers. Ordering of undiluted rods with aspect ratio x = length/diameter is predicted to occur for $x \gtrsim 6.4$.[29] With $l/2$ as the equivalent rod length[30] and $(4/\pi\nu L)^{1/2}$ as the rod diameter, $x = (\pi\nu L l^2/16)^{1/2}$ or $\nu L l^2 \gtrsim 200$ for ordering.
(29) P. J. Flory, *Proc. Natl. Acad. Sci. U.S.A.* **79**, 4510 (1982).
(30) P. J. Flory, *Macromolecules*, 11, 1141 (1978).
(31) G. Ronca, *J. Chem. Phys.* **79**, 1031 (1983).
(32) D. C. Prevorsek and B. T. De Bona, *J. Macromol. Sci., Phys.*, **B19**, 605 (1981).
(33) M. Doi and S. F. Edwards, *J. Chem. Soc., Faraday Trans. 2*, **74**, 1789, 1802 (1978).
(34) W. W. Graessley, *J. Polym. Sci., Polym. Phys. Ed.*, **18**, 27 (1980).
(35) I. D. Rudin, "Poly(1-butene)—Its Preparation and Properties", Gordon and Breach, New York, 1968.
(36) N. Hadjichristidis, X. Zhongde, L. J. Fetters, and J. Roovers, *J. Polym. Sci., Polym. Phys. Ed.*, **20**, 743 (1982).
(37) J. Mays, N. Hadjichristidis, and L. J. Fetters, *Macromolecules*, **1984**, *17*, 2723.
(38) C. J. Stacy and R. L. Arnett, *J. Phys. Chem.*, **77**, 78 (1973).
(39) W. W. Graessley, *Macromolecules*, **15**, 1164 (1982).

Structural Studies of Semifluorinated *n*-Alkanes. 1. Synthesis and Characterization of $F(CF_2)_n(CH_2)_mH$ in the Solid State

John F. Rabolt,* Thomas P. Russell, and Robert J. Twieg

IBM Research Laboratory, San Jose, California 95193. *Received March 16, 1984*

ABSTRACT: A series of semifluorinated *n*-alkanes, $F(CF_2)_n(CH_2)_mH$, has been synthesized as models for semiflexible polymers. In addition to the melting endotherm, DSC measurements indicate the presence of solid–solid phase transitions. Characterization of the molecular structure and the packing of chains in the crystal lattice in the room-temperature phase has been carried out by Raman spectroscopy, small-angle X-ray scattering (SAXS), and wide-angle X-ray diffraction (WAXD). Several possible packing structures consistent with these measurements are discussed.

Introduction

Fluorocarbon homopolymers have generated considerable interest due to their unique thermal, mechanical, and dielectric properties but little emphasis has been placed on characterization since fluoropolymers are usually insoluble in most common solvents and often crystallize in extended-chain morphologies, thus rendering them uncharacterizable by most common techniques.

Simultaneous optimization of the thermal and dielectric properties while attempting to improve the mechanical and solution characteristics has led to the copolymerization of fluorocarbon monomers with their hydrocarbon analogues. Thus, poly(vinylidene fluoride),[1] $(-CF_2CH_2-)_x$, and an E–TFE alternating copolymer,[2,3] $(-CF_2CF_2CH_2CH_2-)_x$, have become commercially available and possess high temperature stability, outstanding mechanical and dielectric properties and are soluble in a number of solvents. A variety of techniques have since been used to study the structure of these copolymers and a significant amount of information has been published detailing their structure in the solid state and in solution.[4–7] Similarly, theoretical studies[8,9] have also appeared using semiempirical atom–atom potentials to calculate minimum energy structures for both an isolated chain and the crystal lattice.

Unlike *n*-alkane oligomers, very few studies have been made of fluorocarbon oligomers because of the lack of availability of a series of high-purity materials. Dipole moments and conformational parameters for a series of α,ω-dihydroperfluoro-*n*-alkanes, $H(CF_2)_nH$ with n = 4, 6, 7, 8, and 10, were reported by Bates and Stockmayer[10] and later[11] expanded to include longer chains and $H(CF_2)_nI$ with n = 4, 6, and 8. Infrared and Raman studies[12,13] of short-chain perfluoro-*n*-alkanes, $F(CF_2)_nF$ with n = 4–6, have appeared while Raman studies[14,15] of the intermediate chain lengths have also been reported. As in the case of *n*-alkanes, the position of certain vibrational bands in perfluoro-*n*-alkanes was observed to vary as a function of chain length and thus was used to plot out portions of the phonon dispersion curves.[16] An overlay force field was then refined by using the finite molecule data and then applied

0024-9297/84/2217-2786$01.50/0